

The magnetic properties of C-Ni carbon-metal complexes

V. V. Chabanenko, E. E. Zubov, A. Nabialek, R. O. Kochkanjan, R. Escudero, F. Morales, F. Pérez-Rodríguez, S. Zolotar, and R. Puźniak

Citation: *Low Temperature Physics* **43**, 625 (2017); doi: 10.1063/1.4985218

View online: <https://doi.org/10.1063/1.4985218>

View Table of Contents: <http://aip.scitation.org/toc/ltp/43/5>

Published by the [American Institute of Physics](#)

Articles you may be interested in

[Emulating rough flux patterns in type-II superconducting cylinders using the elliptic critical-state model](#)
Journal of Applied Physics **122**, 143904 (2017); 10.1063/1.4994905

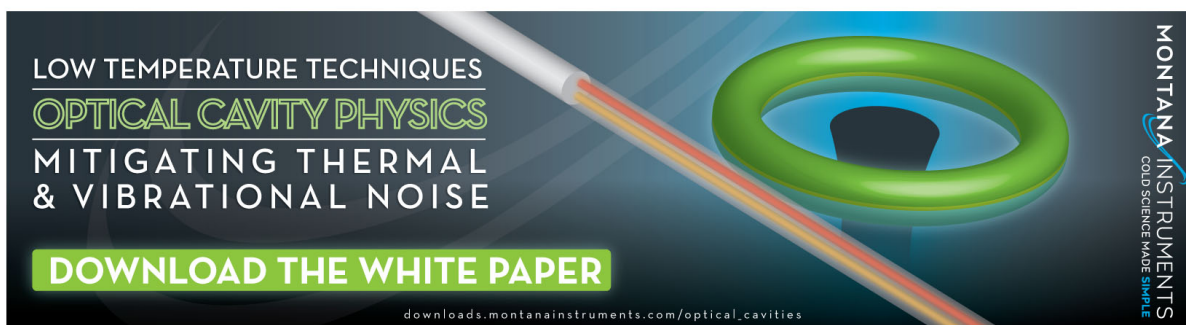
[Electronic structure and x-ray magnetic circular dichroism in \$A_2CrB'O_6\$ \(\$A=Ca, Sr\$; \$B'=W, Re, Os\$ \) oxides](#)
Low Temperature Physics **43**, 578 (2017); 10.1063/1.4985207

[Rotational magnetocaloric effect in \$TbAl_3\(BO_3\)_4\$](#)
Low Temperature Physics **43**, 631 (2017); 10.1063/1.4985220

[Singular optics of spin waves in a two-sublattice antiferromagnet with uniaxial magnetic anisotropy](#)
Low Temperature Physics **43**, 564 (2017); 10.1063/1.4985212

[Proximity effects in multiband superconductor–ferromagnetic metal structures](#)
Low Temperature Physics **43**, 602 (2017); 10.1063/1.4985298

[Low-temperature absorption spectra and electron structure of \$HoFe_3\(BO_3\)_4\$ single crystal](#)
Low Temperature Physics **43**, 610 (2017); 10.1063/1.4985208



LOW TEMPERATURE TECHNIQUES
OPTICAL CAVITY PHYSICS
MITIGATING THERMAL
& VIBRATIONAL NOISE

DOWNLOAD THE WHITE PAPER

downloads.montanainstruments.com/optical_cavities

MONTANA INSTRUMENTS
COLD SCIENCE MADE SIMPLE

The advertisement features a dark background with a glowing green ring and a white rod with a red and orange gradient. The text is arranged in a clean, professional layout.

The magnetic properties of C-Ni carbon-metal complexes

V. V. Chabanenko^{a)}

Galkin Donetsk Physico-Technical Institute of NAS of Ukraine, 46 Nauka Ave, Kiev 03680, Ukraine

E. E. Zubov

Kurdyumov Institute of Metal Physics, NAS of Ukraine, 36 Academician Vernadsky Blvd, Kiev 03680, Ukraine

A. Nabialek

Institute of Physics, PAS, 32/46, al. Lotników, Warsaw 02–668, Poland

R. O. Kochkanjan

Litvinenko Institute of Physical-Organic Chemistry and Coal Chemistry, NAS of Ukraine, 50 Kharkovskoye Hwy., Kiev 02160, Ukraine

R. Escudero and F. Morales

Instituto de Investigaciones en Materiales, Universidad Nacional Autónoma de México, Mexico City, DF, Mexico

F. Pérez-Rodríguez

Instituto de Física, Benemérita Universidad Autónoma de Puebla, Apdo. Post. J-48, Puebla, Puebla 72570, Mexico

S. Zolotar

Galkin Donetsk Physico-Technical Institute of NAS of Ukraine, 46 Nauka Ave, Kiev 03680, Ukraine

R. Puźniak

Institute of Physics, PAS, 32/46, al. Lotników, Warsaw 02–668, Poland

(Submitted April 23, 2017)

Fiz. Nizk. Temp. **43**, 782–788 (May 2017)

A new method of graphite metallization by clusters of metallic atoms is used to produce carbon-metal C-Ni nanocomplexes. Measurements of the magnetic properties of the samples reveal a highly non-equilibrium behavior of magnetization in cases of cooling in a magnetic field and without. The superparamagnetic particle model is used to explain the behavior of the magnetic properties of the nanocomplexes. The anisotropy is determined and the size of the nanoparticles is estimated based on this model. *Published by AIP Publishing.* [<http://dx.doi.org/10.1063/1.4985218>]

1. Introduction

Carbon continues to amaze the world with its large number of allotropic structural modifications. The discovery of one such modification, fullerene, was acknowledged by the Nobel Prize, and its compounds with alkali metals have been endowed with superconducting properties.^{1,2} Fullerene complexes with transition metals (C₆₀Fe, C₆₀Co) exhibit superparamagnetic properties.^{3,4}

A well-known and extensively studied configuration of carbon atoms known as graphite is one of the most stable forms of carbon under standard conditions. The structure of graphite is inherently simple. It consists of layered sheets formed by hexagonal cells. The properties of one such monolayer of carbon atoms, isolated from graphite for the first time using adhesive tape and known as graphene, became another information goldmine in condensed matter physics, and the discovery of graphene was likewise awarded the Nobel Prize.

This new two-dimensional object—graphene, attracted additional attention from researchers who had access to measurement technology with a resolution at the nanoscale level.

The flow of interesting scientific results that determine the properties of this remarkable nanostructural object, as well as the physical phenomena occurring in it, have made it an attractive substance for many new technical applications in nanoelectronics. Its unique mechanical diamond-level strength, excellent mechanical flexibility (elasticity), low friction due to the structural incommensurability of graphene fragments and contacting surfaces,^{5,6} good thermal and high-frequency conductivity that occurs practically without any energy loss, and optical transparency, all make it the most promising substance for many different technical applications.⁷ Examples include transistors, high-speed next-generation amplifiers for mobile phones and satellite communications (at frequencies in the 10 GHz range), ultrasensitive biological sensors, and mobile phone screens. Possible magnetism in graphite (Ref. 8 and references therein) and graphite-based systems can be promising for many applications in the development of nanoscale magnetic devices for spintronics. Of particular interest in graphene-based materials is the ability to control its chemical potential, which allows for the inducement of electron or hole

alloying. This also creates potential opportunities for electrons based on carbon nanoelements.^{9,10}

Carbon films on the surface of metals (Cu, Ni) grow in the form of graphene islets having point defects (carbon vacancies in the carbon structure). The formation of the islets with defects is associated with the incommensurability between the atomic structures of the metal substrate and the graphene sheets. This incommensurability in the case of metal deposition onto graphite crystallites leads to the rejection of the carbon layers (with a thickness of 40–50 nm) from the crystallite and their coagulation into globular formations, as it occurred in C-Co¹¹ and C-Cu complexes. On the periphery of these formations there is a multi-walled graphene layer and in the central part is a clustered metal core. This type of detachment of the graphene layers leads, in essence, to structures that are ligand metal clusters.

This article reports on the investigations of the magnetic properties of carbon-metal C-Ni nanocomplexes obtained by metallization of specially prepared (sensitized) graphite by nickel nanoclusters. The measurement of the magnetic properties of the samples reveals a highly non-equilibrium behavior of magnetization during measurement in cases of cooling in a magnetic field (FC) and without (ZFC). The superparamagnetic particle model is used to explain the behavior of the magnetic properties of carbon-metal complexes.

2. Samples and the measurement of their properties

In order to obtain nanostructured C-Ni complexes we used a new method of chemical metallization of graphite. For this, the graphite was preliminarily cleaned of any inorganic substance impurities via a mineral acid treatment and tin salt sensitization. After the stage of sensitization the graphite was activated by silver or palladium salts. Metal clusters were obtained by reducing the corresponding salts in aqueous solutions by various reducing agents such as hydrazine, sodium hypophosphite, sodium borohydride and formaldehyde. The synthesis temperature was in the range of 20–90 °C. The obtained complexes had a flat powdery structure. The nanostructured metal complex powder C_{5.28}O_{8.89}PNi_{1.83}Fe_{0.02} was pressed into a strip having the dimensions 1 × 0.4 × 0.07 cm so that magnetic research could be conducted. The molar mass of the substance was 345.15 g/mol. The presence of phosphorus in the given material is the result of the synthesis characteristics and does not affect the magnetic properties of the substance.

Measurements of the temperature dependences of magnetization in FC and ZFC cooling modes were performed using a vibratory Foner magnetometer. The magnetic properties in an alternating magnetic field \tilde{h} were studied using a PPMS setup. In this case the sample had the shape of a disk with a diameter of 5 mm and a thickness of 0.7 mm (mass $m = 26.8$ mg) and it was placed into a coil that created an alternating field with a frequency of 10–10⁴ Hz. The alternating magnetic field, like a constant external field, was directed perpendicular to the surface of the disk.

3. The results of the magnetic measurements and their analysis

Figure 1(a) shows the experimental temperature dependences of equilibrium (FC) and non-equilibrium (ZFC) magnetization

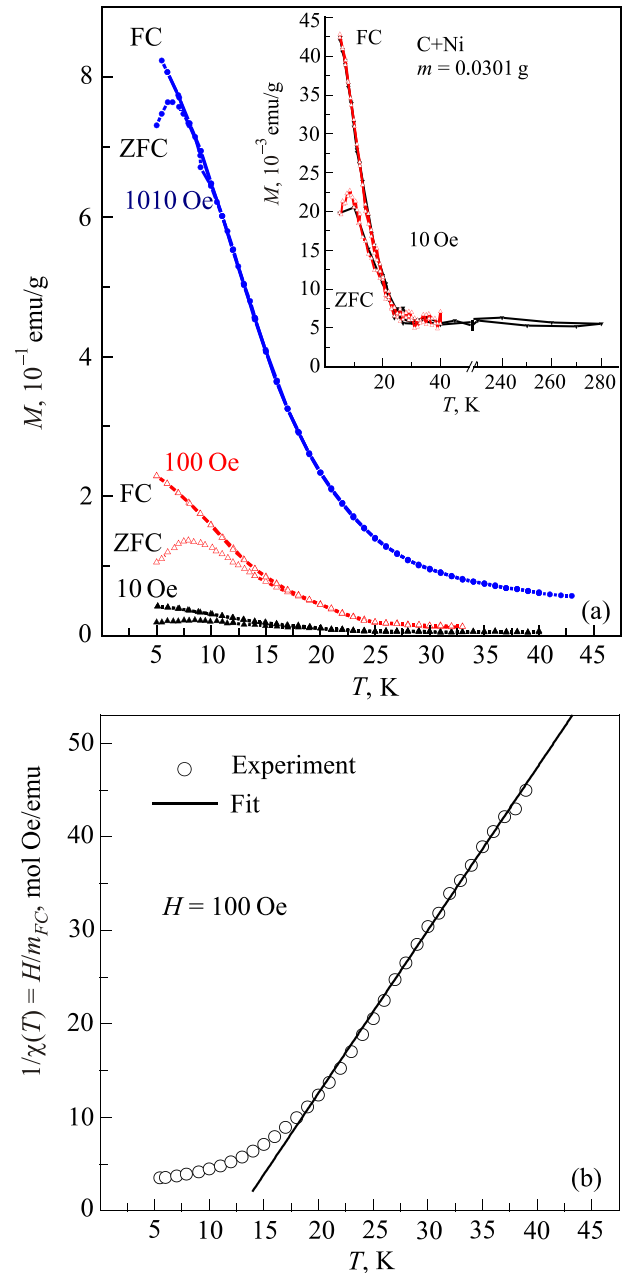


Fig. 1. The experimental temperature dependences of magnetization M_{FC} and M_{ZFC} of the C-Ni metal complex under various external magnetic fields. The inset shows the temperature dependences of the magnetization over a broad temperature range (a); reverse magnetization as a function of temperature (b).

of the metal complex in magnetic fields of 10, 100, and 1010 Oe. As shown on the inset, the metal complex is a paramagnet up to a temperature of 40 K. Then, at lower temperatures there is a magnetic phase transition. Based on the data presented, equilibrium high-temperature susceptibility m_{FC}/H in a field $H = 100$ Oe, using the Curie law can be written as

$$\chi(T) = \frac{C}{T - \theta}, \quad (1)$$

where $C = \frac{1}{3k_B} \mu_{\text{eff}}^2$ is the Curie constant, k_B is the Boltzmann constant, $\mu_{\text{eff}}(S) = \mu_B n_{\text{eff}}$ is the effective magnetic moment, $n_{\text{eff}} = g \sqrt{S(S+1)}$ is the effective number of Bohr magnetons and θ is the paramagnetic Curie temperature, and based on the linear fitting for $1/\chi(T) = H/m_{FC}(T)$ over the temperature

range 17 K–36 K, the values $C = 0.575$ emu K/mol and $\theta = 12.8$ K were obtained [see Fig. 1(b)]. From this we can derive the effective number of Bohn magnetons $n_{\text{eff}} = 2.14$ which for $g = 2$ gives us the effective spin of $S_{\text{eff}} = 0.68$. The small value of the Curie constant and the value of the effective number of Bohr magnetons correspond to the magnetic moment of the nickel ion¹² in organometallic compounds and indicate that the cluster properties of the compound are not manifested in the temperature range under study. The sign of the paramagnetic temperature also points to the ferromagnetic nature of the magnetic interactions.

Figure 1(a) also shows that the non-equilibrium effects appear below the temperature of 15 K, i.e., almost immediately after the magnetic ordering of the superparamagnetic particles in the system. In order to determine their characteristic dimensions, as well as their anisotropy field, we will use the simplest spherical particle model with a magnetic moment M_{cl} , volume V , and uniaxial anisotropy with the constant K . We will write the expression for energy E of the particle in a magnetic field as

$$E = K \sin^2 \theta - M_{\text{nr}} V H \cos \theta, \quad (2)$$

wherein $M_{\text{nr}} = M_{\text{cl}}/V$ is the magnetization, and θ is the angle between the moment of the particle and the magnetic field that is directed along the z axis. For simplicity we will assume that the anisotropy axes of the particles are parallel to the z axis. Taking into account the form of Eq. (2) for the particle energy it is easy to write down the expression for the magnetization $M(H)$ of the whole sample¹³

$$M(H) = \frac{M_{\text{nr}}}{Z(\alpha, \beta)} \int_0^\pi d\theta \exp(-\alpha \sin^2 \theta + \beta \cos \theta) \cos \theta \sin \theta, \quad (3)$$

wherein $\alpha = H_c M_{\text{cl}} / (2k_B T)$, $\beta = M_{\text{nr}} V H / (k_B T)$ and $H_c = 2KV / M_{\text{cl}}$ is the anisotropy field,

$$Z(\alpha, \beta) = \int_0^\pi d\theta \exp(-\alpha \sin^2 \theta + \beta \cos \theta) \sin \theta. \quad (4)$$

The integrals in Eqs. (3) and (4) can be easily written using the Dawson function $F(x)$, which is directly related to the imaginary part of the error function $\text{erf}(x)$ by the expression $F(x) = -(i\sqrt{2}/2)e^{x^2} \text{erf}(ix)$. As such, we can write the following expression for the magnetization of the sample:

$$M(H) = \frac{T}{H_c V} \frac{\sqrt{\alpha}(e^{2\beta} - 1) + \beta F\left(\frac{\beta - 2\alpha}{2\sqrt{\alpha}}\right) - \beta e^{2\beta} F\left(\frac{\beta + 2\alpha}{2\sqrt{\alpha}}\right)}{e^{2\beta} F\left(\frac{\beta + 2\alpha}{2\sqrt{\alpha}}\right) + F\left(\frac{2\alpha - \beta}{2\sqrt{\alpha}}\right)}. \quad (5)$$

The given formula depends on 3 unknown parameters: M_{cl} , V , and H_c . However it is possible to reduce the number of the unknowns to two, if we consider the following connection between the blocking temperature T_B , the magnetic moment of the particle M_{cl} , and the coercivity field $H_{\text{coer}}(T)$ at temperature T :

$$H_{\text{coer}}(T) = H_c \left(1 - \sqrt{\frac{T}{T_B}}\right) p, \quad (6)$$

wherein p is the averaging coefficient that shows the degree of disorder of the anisotropy axes of the magnetic particles with respect to the direction of the external magnetic field H . In the case of a random distribution of the anisotropy axes' direction $p \sim 0.5$.¹⁴

We can see in Fig. 2(a) that at $T = 5$ K the value of the coercivity field is $H_{\text{coer}}(T) = 290$ Oe. The experimental value of the blocking temperature that corresponds to the ZFC magnetization maximum in a field $H = 100$ Oe is equal $T_B = 7.9$ K [Fig. 1(a)]. Therefore at $p \sim 0.5$ based on Eq. (6) we obtain the anisotropy field $H_c = 2833$ Oe. The result of fitting the calculated dependence of magnetization (5) to the experimental values $M(H)$ [dots on Fig. 2(b)] is presented in Fig. 2(b) (line) at particle volume $V = 4.88 \times 10^{-20}$ cm³ and its magnetic moment $M_{\text{cl}} = 2 \times 10^{-19}$ emu. From this we get the saturation magnetization $M_{\text{nr}} = 4.1$ emu/cm³ (or 3.82 emu/g) which is achieved in magnetic fields of more than 11 T. Knowing the

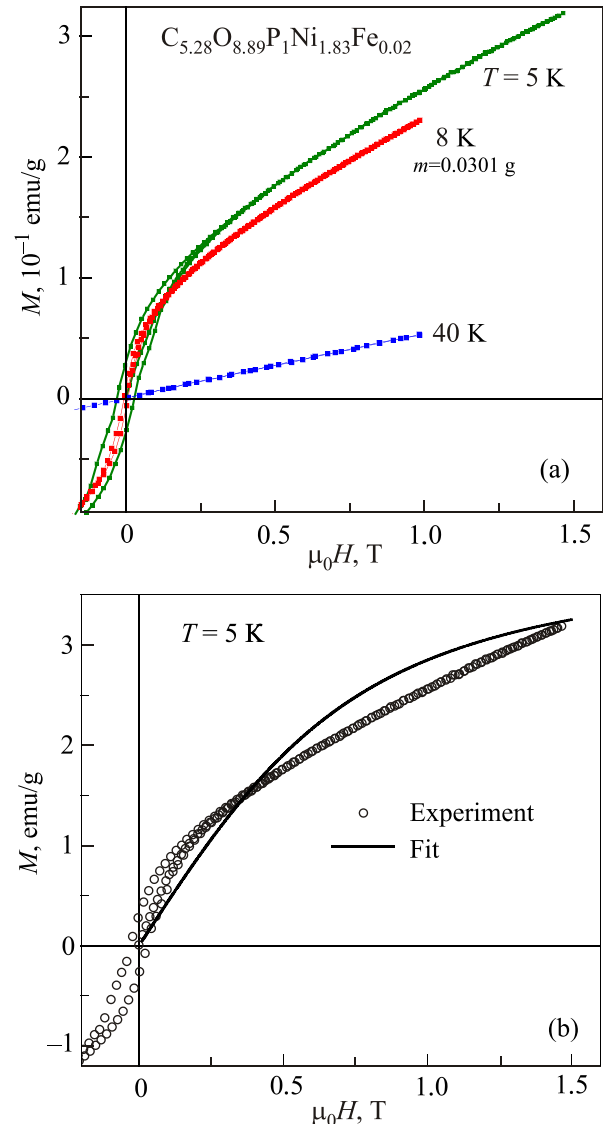


Fig. 2. The field dependence of magnetization of the C-Ni metal complex at various temperatures (a); approximation of the experimental curve $M(H)$; $T = 5$ K (b).

volume V we obtain the characteristic radius for nanoparticles in the form of a sphere: $R_{cl} = (3V/4\pi)^{1/3} = 22.7 \text{ \AA}$.

Let us investigate the frequency properties with respect to the phenomena of non-equilibrium magnetism of this compound. According to Néel relaxation theory,¹⁵ there is a simple relationship between the blocking temperature and the anisotropy energy of the particle. In our case at $\tau_0 = 1/\gamma_0$ and for the characteristic measurement time $t_m = 50 \text{ s}$, the following relation should be approximately satisfied:

$$20k_B T_B / KV \sim 1. \quad (7)$$

For the parameters obtained above, this ratio is $20k_B T_B / KV \sim 77$, which is almost two orders of magnitude greater than 1. Such a contradiction has been repeatedly noted in different research studies^{16,17} and is associated with the fact that it is necessary to account for the interaction between magnetic particles. Accounting for this interaction leads to a modification of the Arrhenius law $\tau = \tau_0 e^{KV/(k_B T)}$ for the relaxation time, where $\tau_0 \sim 1/\gamma_0 \sim 6 \times 10^{-8} \text{ s}$ and γ_0 is the gyromagnetic ratio. When the characteristic energy $k_B T_0$ of nanoparticle interaction is significantly greater than the anisotropy energy, the effective field of particle interaction is added to the anisotropy field. Then for the relaxation time it is necessary to use the Vogel-Fulcher expression:¹⁷

$$\tau = \tau_0 \exp\left(\frac{KV}{k_B(T - T_0)}\right). \quad (8)$$

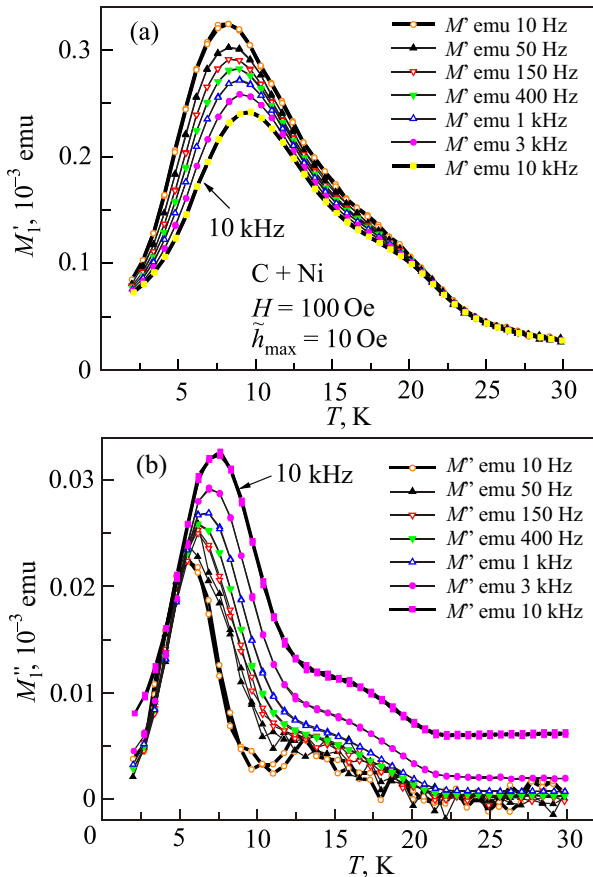


Fig. 3. The temperature dependences of the real (a) and imaginary (b) parts of the first harmonic of the C-Ni metal complex magnetization at various measurement frequencies; ZFC, $H = 100 \text{ Oe}$; $h_{\max} = 10 \text{ Oe}$.

In the case of $k_B T_0 \gg KV$ the volume V in Eq. (8) becomes temperature-dependent due to nanoparticle correlation, i.e., it is transformed into V_{eff} (Ref. 17)

$$V_{\text{eff}} = VT_0 / (T - T_0). \quad (9)$$

In this case the relaxation time is written as

$$\tau = \tau_0 \exp\left(\frac{KV}{k_B T} \sqrt{\frac{T_0}{T - T_0}}\right). \quad (10)$$

Taking into account the experimental value of the blocking temperature we can estimate the T_0 according to formula

$$T_0 = T_B \left\{ 1 + \left(\frac{KV}{k_B T_B \ln(100/\tau_0)} \right)^2 \right\}^{-1}, \quad (11)$$

which [due to the smallness of the second term in (11)] is practically the same as T_B . Therefore, in our case a more complex relationship $T_0 \sim KV/k_B$ is realized, which does not correspond to the limiting cases (8) and (10) for the relaxation times. Therefore, in order to analyze the frequency dependences of the magnetic moment close to the blocking temperature we take an average of the effective nanoparticle volume as $V_{\text{eff}} = 30 \text{ V}$, which allows us to approximately satisfy Eq. (7). The given assumption does not contradict

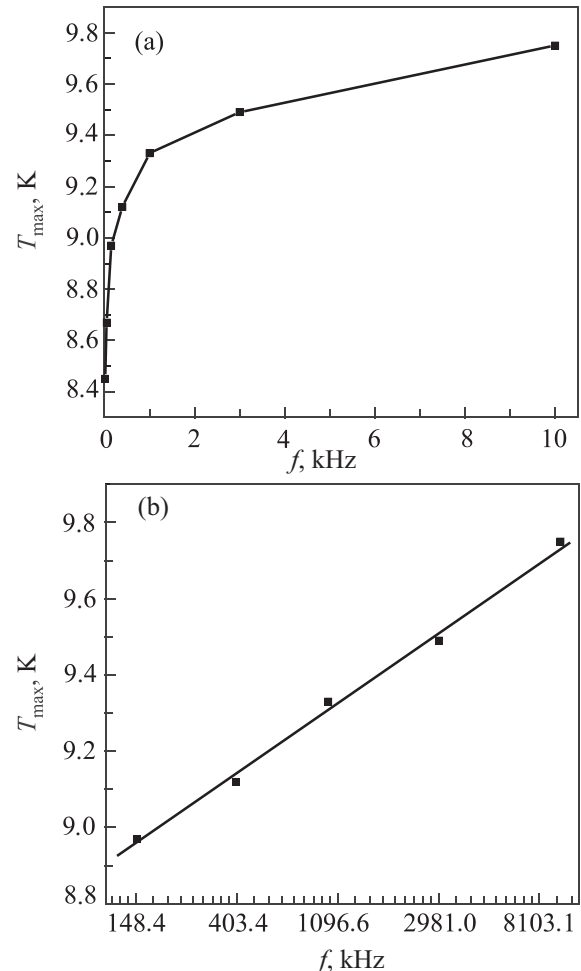


Fig. 4. The dependence of the position of the maximum of the real part of magnetization on the temperature and frequency axes $T_{\max}(f)$ in linear (a) and logarithmic (b) scales.

Eq. (6) for the coercivity field, since its experimental value is obtained when the magnetic field decreases from large values, as is usually necessary for the hysteresis loop to be constructed. In this case the particle interaction is blocked, which points to low values of the field $H_{coer}(T)$.

Figure 3 shows the temperature dependences of the real (a) and imaginary (b) parts of the first harmonic of the C-Ni metal complex magnetization at various measurement frequencies of an alternating magnetic field. The frequency dependence of the positions of the maxima $T_{max}(\omega)$ could be indicative of both a spin-glass and superparamagnetic behavior. Within the framework of the spin-glass model with $\tau = \tau_0 \exp(F_B/T)$ for $T = T_{max}(\omega)$ and

$$1/T_{max}(\omega) = -(\ln \omega + \ln \tau_0)/F_B \quad (12)$$

it is possible to estimate the values of the potential barrier F_B and the typical relaxation time τ_0 .

Figure 4 shows the experimental dependence $T_{max}(\omega)$ (a) and the result of fitting the dependence according to Eq. (12) (b). As a result of this an anomalously high value of $F_B = 430.7$ K is obtained as is an unnaturally small characteristic relaxation time $\tau_0 = 7.3 \times 10^{-24}$ s. It appears that in our case the superparamagnetism model is in action. In order to confirm this assumption we estimate the frequency properties, relying on the above-defined microscopic interaction parameters within the framework of this model.

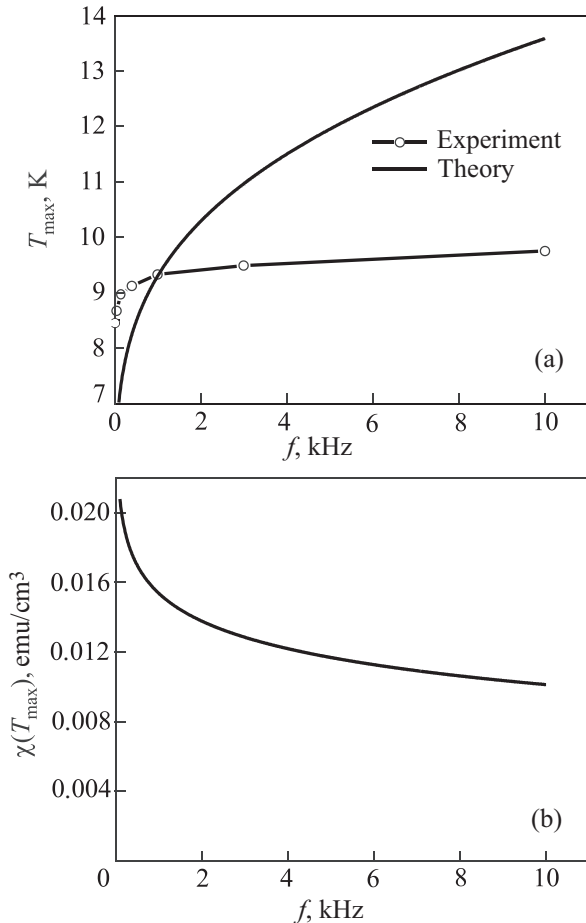


Fig. 5. The frequency dependences of the position of the maximum $T_{max}(f)$ and the magnitude of the real part of the complex susceptibility $\chi(T_{max})$ at the maximum (b).

In order to determine the susceptibility of the system we will use Brown's model,¹⁸ which allows us to calculate the number of particles having a magnetic moment along and against the direction of the anisotropy axis, with consideration of the existing barrier. By adding the values $\pm v e^{i\omega t}$ that are caused by the inclusion of the weak alternating magnetic field $h_0 e^{i\omega t}$ to the already-known probabilities of particle transitions from one state to another, it is easy to obtain the following expression for complex susceptibility:

$$\chi(\omega) = \frac{M_{nr}^2 V_{eff}}{k_B T (1 + i\omega\tau)}, \quad (13)$$

wherein for τ the Arrhenius law with $V_{eff} = 30$ V is fulfilled. It is obvious that the real part of $\chi'(\omega)$ susceptibility assumes the form

$$\chi'(\omega) = \frac{M_{nr}^2 V_{eff}}{k_B T (1 + \omega^2 \tau^2)}. \quad (14)$$

The maximum $T_{max}(\omega)$ of the susceptibility (14) is defined by the transcendental function

$$\frac{2KV_{eff}\omega^2\tau^2}{k_B T \left(\exp\left(-\frac{2KV_{eff}}{k_B T}\right) + \omega^2\tau^2 \right)} = 1. \quad (15)$$

Figure 5 shows the calculated curve of the susceptibility maximum $T_{max}(\omega)$ position on the temperature axis from (15) (line) and experimental values of the magnetization maxima from Fig. 3(a). It can be seen that there is a qualitative correspondence between theory and experiment. Likewise based on the calculated dependence $\chi'(T_{max})$ [Fig. 3(b)] it follows that as the frequency increases, the amplitude of the maxima drops, which corresponds to the results of the experiment on Fig. 3(a).

The frequency dependences (experimental and calculated) of the susceptibility maximum of a carbon-metal C-Ni complex are shown in Fig. 6 on a logarithmic scale. Here the experimental curve is made of dots, and the dot-dashed line shows the calculated curve. The certain difference in the

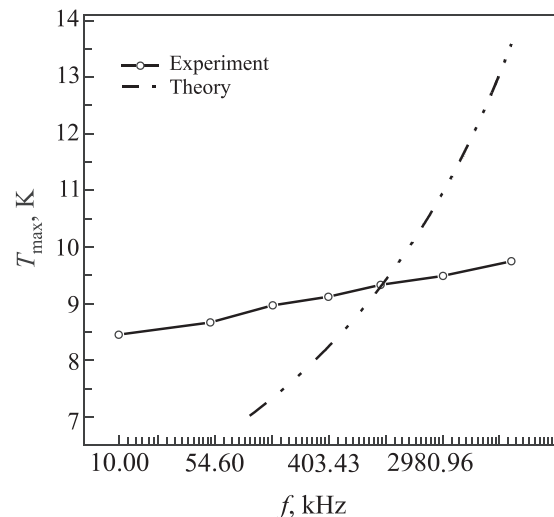


Fig. 6. The frequency dependences of the susceptibility maximum in a logarithmic scale: experimental (dots) and calculated (dot-dashed curve).

slopes of the curves indicates the approximate nature of the chosen model which does not account for the magnetic interaction complexes in the nanostructured C-Ni powder.

4. Conclusion

Carbon-metal nanocomplexes C-Ni were obtained by metalizing graphite with clusters of metallic atoms. The material had a highly non-equilibrium magnetization behavior during cooling in a magnetic field (FC) and without (ZFC). The superparamagnetic particle model was used to explain the behavior of the magnetic properties of these nanocomplexes. The anisotropy was determined and the characteristic particle size was estimated within the framework of this model.

R. Escudero and F. Morales acknowledge support from UNAM GRANT IT100217 and are grateful to A. Lopez and A. Pompa-Garcia.

^{a)}Email: vikchabanenko@gmail.com

¹H. W. Kroto, J. R. Heath, S. C. O'Brien, R. F. Curl, and R. E. Smalley, *Nature* **318**, 162 (1985).

²A. F. Hebard, M. J. Rosseinsky, R. C. Haddon, D. W. Murphy, S. H. Glarum, T. T. M. Palstra, A. P. Ramirez, and A. R. Kortan, *Nature* **350**, 600 (1991).

³V. Chabanenko, E. Zubov, P. Byszewski, L. Gladczuk, and E. Kowalska, *J. Magn. Magn. Mater.* **249**, 475 (2002).

⁴E. Zubov, P. Byszewski, V. Chabanenko, E. Kowalska, L. Gladczuk, and R. Kochkanjan, *J. Magn. Magn. Mater.* **222**, 89 (2000).

⁵M. Dienwiebel, G. V. Verhoeven, N. Pradeep, J. W. M. Frenken, J. A. Heimberg, and H. W. Zandbergen, *Phys. Rev. Lett.* **92**, 126101 (2004).

⁶X. Feng, S. Kwon, J. Y. Park, and M. Salmeron, *ACS Nano* **7**, 1718 (2013).

⁷See <http://phys.org/news/2016-03-electricity-graphene-highfrequencies-energy.html#jCp>

⁸J. Červenka, M. I. Katsnelson, and C. F. J. Flipse, *Nat. Phys.* **5**, 840 (2009).

⁹T. Ma, S. Liu, P. Gao, Z. B. Huang, and H. Q. Lin, *J. Appl. Phys.* **112**, 073922 (2012).

¹⁰T. Ma, F. Hu, Z. Huang, and H. Q. Lin, *Appl. Phys. Lett.* **97**, 112504 (2010).

¹¹V. V. Chabanenko, E. E. Zubov, R. Cortés-Maldonado, F. Pérez-Rodríguez, R. Escudero, F. Morales, R. Kochkanjan, O. Kuchuk, and A. Nabialek, in XXIII International Materials Research Congress on Magnetic Properties of Nanostructured C-Co Complexes, *IMRC XXIII*, Cancun, Mexico, 17–21 August (2014), p. 10.

¹²E. König, "Magnetic properties of coordination and organometallic transition metal compounds," in *Landolt-Börnstein, Group II Molecules and Radicals* (Springer, 1966), Vol. 2.

¹³J. L. Dormann, D. Fiorani, and E. Tronc, *Adv. Chem. Phys.* **98**, 283 (2007).

¹⁴E. C. Stoner and E. P. Wohlfarth, *Philos. Trans. R. Soc. London A* **240**, 599 (1948).

¹⁵C. P. Bean and J. D. Livingston, *J. Appl. Phys.* **30**, 120 (1959).

¹⁶J. A. Mydosh, *Spin Glasses: An Experimental Introduction* (Taylor and Francis, London, Washington, 1993).

¹⁷S. Shtrikman and E. P. Wohlfarth, *Phys. Lett. A* **85**, 467 (1981).

¹⁸W. F. Brown, *Phys. Rev.* **130**, 1677 (1963).

Translated by A. Bronskaya